

Article

# Sensitivity of EGFR/HER-2 Positive Cells Isolated from Ascitic Fluid of Advanced Ovarian Cancer Patients to EGFR/HER-2 Inhibitors

Kenny Chitcholtan \*, Dianne Harker, Bryony Simcock and Peter Sykes

Gynaecological Cancer Research Group, Department of Obstetrics and Gynaecology, University of Otago, Christchurch 8140, New Zealand; dianne.harker@otago.ac.nz (D.H.); bryony.simcock@cdhb.govt.nz (B.S.); peter.sykes@otago.ac.nz (P.S.)

\* Correspondence: kenny.chitcholtan@otago.ac.nz; Tel.: +64-21-025-35924

Received: 2 March 2020; Accepted: 23 March 2020; Published: 29 March 2020



**Featured Application:** Targeted inhibitor in ovarian cancer treatment.

**Abstract:** Background: advanced ovarian cancer often presents with ascites. These ascites contain small clusters of cancer cells, which may contribute greatly to the metastatic potential of ovarian cancer in the peritoneal cavity. Therefore, understanding the unique protein expressions of this cell population will provide vital information for the development of tailored, targeted treatment. In this study, we isolate floating ovarian cancer cells from ovarian cancer patient ascitic fluid and use these cells to document that the expression of EGFR/HER-2 proteins may be essential for the growth and survival of these floating cancer cell clusters. Methods: ascitic fluid-derived cells were isolated from ascitic fluid by using Ficoll separation. Cells were cultured in a non-adherent condition for six days. The protein level of EGFR, HER-2, AKT, and ERK and their phosphorylation in ovarian cancer cell lines were determined by immunofluorescence. The immunofluorescent staining for proteins presented in ascitic fluid-derived cells determined the intensity profile of each protein using Carl Zeiss Blue software. Results: Isolated ovarian cancer cells from ascitic fluid have a measurable level of EGFR and HER-2 proteins. The inhibition of EGFR and EGFR/HER-2 positive cells with gefitinib and canertinib selectively disrupts cell viability and the protein level of EGFR, HER-2, AKT and ERK and their respective phosphorylation status. In addition, the dual EGFR/HER-2 inhibitor canertinib demonstrates greater anti-tumour effects than gefitinib in EGFR/HER-2 positive cells. Conclusion: These studies reveal an important role of multiple activation of receptor tyrosine kinases in floating ovarian cancer cells, as well as the importance of a dual EGFR/HER-2 inhibitor used as alternative adjuvant therapy in advanced ovarian cancer patients.

**Keywords:** ovarian cancer; cell clusters; EGFR; HER-2; gefitinib; canertinib; ascitic fluid

## 1. Introduction

About 35% of patients with advanced ovarian cancer have ascitic fluid present at initial diagnosis and during the course of treatment [1]. Ascites is positively correlated with a poor prognosis, chemoresistant tumour features and deterioration in the patient's quality of life [2,3]. Ascitic fluid contains biological components including cytokines, chemokines, growth factors, small molecules, white blood cells, mesenchymal cells and ovarian cancer cells [4–6]. Therefore, this unique microenvironmental milieu within the peritoneal cavity may promote tumour cell growth and modulate tumour cells responding to chemotherapy.

The dissemination of ovarian cancer cells occurs at an early stage of the disease. Tumour cells detach from the primary tumour; many form small clusters and move around in the peritoneal cavity

with the movement of the peritoneal fluid [7,8]. In addition, increasing numbers of these cell clusters are found in the ascitic fluid of the advanced disease [9,10]. Genotypic and phenotypic signatures of these floating cancer cells are poorly understood. However, it is widely recognised that these cancer cells are the major source of secondary metastasis growth [11]. Therefore, acknowledging the unique phenotypic features, associated with certain oncogenic proteins of the floating cancer cells, is necessary to understand the biology of metastasising ovarian cancer. The identification of specific proteins that may have oncogenic potential and that can be inhibited with existent clinical drugs may offer clinical benefits to a subset of ovarian cancer patients.

It is widely recognised that tumour cells manifest rapid growth and sustained survival processes, which are facilitated by oncogenic protein-specific pathways. Elevated levels of the protein family of epidermal growth factor receptors, including EGFR and HER-2 in tumour tissue, have been linked with the poor prognosis of women with advanced ovarian cancer [12–14]. The activation of EGFR and HER-2 has been well documented in several solid tumours, in which the receptors were crucial to sustain growth and survival during the course of chemotherapy treatment [15–17]. Many *in vitro* studies and preclinical models have also demonstrated the effectiveness of EGFR and HER-2 inhibitors in delaying growth, reducing cancer cell survival and the metastatic potential of ovarian cancer [18–20]. Furthermore, the combination of these targeted inhibitors with standard cytotoxic agents have demonstrated enhanced anti-tumour activities compared with mono treatments [21].

Even though the expression of these receptors in ovarian tumour tissues has been well described, the role they play in metastasis and chemoresistance is still poorly understood. Investigating the receptors' status in cells derived from ascites from ovarian cancer patients will somewhat delineate this role. In addition, the efficacy of EGFR and HER-2 inhibitors has not yet been studied in these types of cells. In this study, we hypothesised that cells isolated from ascitic fluid will have detectable expression levels of EGFR and HER-2, and in turn the efficacy of the inhibitor will be notable in these EGFR and HER-2 positive cells.

## 2. Materials and Methods

### 2.1. Cell Lines

Three ovarian cancer cell lines; OVCAR-5, SKOV-3 and OVCAR-4, were obtained from Dr Judith McKenzie, Haematology Research Group, University of Otago, Christchurch, New Zealand. OVCAR-5, SKOV-3 and OVCAR-4 cells were maintained in DMEM media (GIBCO<sup>®</sup>, Life Technologies, Auckland, New Zealand), supplemented with 10% foetal bovine serum (FBS) (GIBCO<sup>®</sup>, Life Technologies, New Zealand), Pen/Strep (GIBCO<sup>®</sup>, Life Technologies, New Zealand) at a working concentration of 100 units/mL penicillin, 100 units/mL streptomycin, 2 mM glutaMAX<sup>™</sup> (GIBCO<sup>®</sup>, Life Technologies, New Zealand) and 1 µg/mL Fungizone (Life Technologies, New Zealand). The final concentration of glucose in the media was 5.5 mM. The respective supplemented media is henceforth referred to as working media. Cells were maintained at 37 °C in a humidified 5% CO<sub>2</sub> atmosphere. SKOV-3 and OVCAR-5 cell lines were authenticated using short tandem repeat (STR) testing by CellBank (Children's Medical Research Institute, New South Wales, Australia).

### 2.2. Isolation of Cells from Ascitic Fluids

Ascitic fluids from advanced ovarian cancer patients were collected during debulking surgery and paracentesis at the Department of Obstetrics and Gynaecology and the Medical Day Unit (MDU), Christchurch Women's Hospital. Patient consent was obtained prior to the collection of ascitic fluid. Volumes of 500 to 2000 mL were collected and kept in the fridge not more than 24 h before cell separation. Cellular components were separated from the fluid by centrifugation at 500 g for 10 min. Cell pellets were re-suspended in a phosphate buffer saline (PBS) and re-spun at 400 g for 10 min. Cells were mixed with PBS, and cell separation was carried out by using Ficoll-Paque (EG Healthcare, New Zealand). Cells were spun at 300 g for 40 min, and the top fraction was collected and re-spun at 400 g

for 10 min. Cell pellets were mixed with working media and maintained in cell culture flasks, allowing cells to propagate. Working media was refreshed every two days.

### 2.3. Establishment of Cell Clusters of Ovarian Cancer Cell Lines and Ascitic Fluid-Derived Cells

Ovarian cancer cell lines (200,000) and ascitic fluid-derived cells (20,000 to 50,000) were cultured on Poly-(2-hydroxyethyl methacrylate, Poly-HEMA) precoated 24-well plates, supplemented with 1 mL working media. Cells were allowed to grow for six days and synchronised in serum-depleted media for 24 h. Then, cells were treated with working media containing 5 $\mu$ M gefitinib and canertinib for 48 h. Control cells contained a similar amount of vehicle dimethyl sulfoxide (DMSO) as present in the inhibitor-stimulated cells.

### 2.4. Measurement of Cellular Viability Using Alamar Blue Dye Assay

After a 24-h incubation of cells with the inhibitors, 100  $\mu$ L of 440  $\mu$ M Alamar Blue dye was added to 1 mL cell suspension, and cells were incubated further for 24 h. Condition media (200  $\mu$ L) from each sample were transferred to a 96-well plate, and the absorbance at 570 and 600 nm was read with a spectrophotometer with a multiple plate reader (Thermofisher Scientific, Auckland, New Zealand). Cellular viability was calculated from the difference of absorbance at 600 and 570 nm. For cell growth activity, cell clusters were collected and incubated with 1Xtrypsin-EDTA for 10 min. The number of cells was counted by haemocytometer.

### 2.5. Immunofluorescence of Cell Clusters

After exposing cells to inhibitors for 48 h, cells were harvested and fixed with ice-cold 50% (v/v) acetone/methanol solution for 40 min at 4  $^{\circ}$ C. After fixing, ascitic fluid-derived cell clusters and OVCAR-5 cell clusters were washed twice with ice-cold PBS, pH 7.4, and re-suspended in 200  $\mu$ L cold PBS. Clusters of cells were then mounted on poly-lysine-coated microscope slides and left to dry at 37  $^{\circ}$ C. Ascitic-derived cell compact aggregates and SKOV-3 aggregates were washed with PBS, pH 7.4, and stained with an aniline blue dye for 20 min. Cells were washed with PBS, pH 7.4, twice before they were embedded in optimal cutting temperature (OCT) compound, an embedding medium used for the sectioning of frozen tissue samples in a cryostat (Thermofisher Scientific, New Zealand). The liquid OCT blocks were frozen at minus 20  $^{\circ}$ C for at least 24 h. Sections (7  $\mu$ m thick) from the block of frozen OCT were cut using a CM186UV Cryostat (Lieca BIOSYSTEM, Wetzlar, Germany). Then, cells on slides were blocked with 4% BSA in 1XPBS for 60 min. Cells were stained overnight with a 1:200 dilution of primary antibody at 4  $^{\circ}$ C. Cells were then washed with ice-cold PBS, pH 7.4. A 1:500 dilution of secondary antibody, conjugated with FITC or Atto-594 nm, was added to cells and further incubated for 60 min. The secondary antibody solution was removed, and 500  $\mu$ L of 10  $\mu$ g/mL DAPI was added to the cells and left for 20 min in the dark. Cells were then washed with 0.1% Tween-20 in PBS, pH 7.4, and were mounted with ice-cold anti-fading solution (2 mg/mL p-phenylenediamine in 80% glycerol, pH 7.8). Immunofluorescent staining was carried out using primary antibodies from Santa Cruz Biotechnology (Santa Cruz, CA, USA). The primary antibodies used in this study were anti-PCNA (sc-25280), anti-GAPDH (sc-25778), anti-EGFR (sc-03), anti-p-EGFR (sc-101668), anti-pHER2 (sc-12352-R), anti-ERK (sc-94), anti-pERK1/2 (sc-7383), anti-AKT (sc-8312), anti-p-AKT (sc-101629), anti-CA125, anti-cytokeratin-18, anti-E-cadherin, anti-N-cadherin and anti-vimentin. The anti-HER-2 was purchased from BD Biosciences (Auckland, New Zealand). Fluorescent images were captured using an epifluorescence microscope with a 40x/1.3 N.A. oil/DIC objective lens (AxioVision 4.5. Apotome software, Carl Zeiss, Oberkochen, Germany). During the capturing of fluorescent images of each protein, the exposure times of immunofluorescent intensity of proteins were similar in both control and drug-treated samples. The intensity profile of each protein was then analysed by a ZEN-blue software, and the profile was expressed as an arbitrary unit (au), which was then normalised to controls of each protein, and the final number was represented as a percentage (%).

## 2.6. Immunoblotting Analysis

Cell clusters and aggregates were harvested by centrifugation at 400 g for 5 min, and the cell pellets were lysed in an ice-cold lysis buffer (20 mM PBS, pH7.4, 100 mM NaCl, 0.1% SDS, 20% glycerol and phosphatase and protease inhibitor cocktail tablets (ThermoFisher, Auckland, New Zealand)). The cell lysates were left on ice for a further 30 min, and a sample buffer (0.2% (v/v) bromophenol blue, 25% (v/v) glycerol, 10% SDS in Tris-HCl, and pH 6.8) was added, and protein lysates were boiled for 10 min. Prior to loading, the cell lysates were mixed and centrifuged at 9700 g for 5 min. A total of 20 µg protein lysate was loaded and separated by SDS-PAGE using a 5% stacking gel and a 10% separating gel. The SDS-PAGE was run at 120 V, using tris-glycine running buffer. The SDS-PAGE markers used were MagicMark™ XP Western Standard (ThermoFisher Scientific, Auckland, New Zealand) and Precision Plus Protein standard (Bio-Rad, Auckland New Zealand). Separated proteins were electroblotted onto a poly-vinyl difluoride (PVDF) membrane (GE Healthcare Life Sciences, New Zealand). The electroblotting was run at 100 V for 60 min in cold tris-glycine running buffer, containing 10% v/v methanol. The membranes were blocked for 60 min, with either 5% (w/v) non-fat skim milk (Pams brand, New World, New Zealand), or 1% (w/v) bovine serum albumin (ThermoFisher Scientific, Auckland, New Zealand), made up in TBS-T buffer or with Pierce Protein-Free Blocking Buffer (ThermoFisher Scientific, New Zealand). Antibodies (detailed above) were diluted from 1:500 to 1:1000, with the appropriate blocking solution. Membranes were incubated with the primary antibodies overnight at 4 °C. The membranes were washed with TBS-T buffer on an orbital shaker for 4 × 10 min and then incubated with a secondary antibody on an orbital shaker for 90 min at room temperature. Membranes were further washed four times with TBS-T. Antibody localisation was determined using a chemiluminescent detection kit (Amersham ECL Prime Western Blotting Detection Reagent Kit, GE Healthcare). The protein bands were visualised, and a densitometry analysis was performed using Alliance 4.7, UNITEC (Cambridge, UK). Cell lysates were collected from at least three separate cell culture experiments. The two secondary antibodies used in this study (purchased from Santa Cruz Biotechnology) were bovine anti-rabbit IgG-HRP (sc-2385) and bovine anti-mouse IgG-HRP (sc-2380).

## 2.7. Statistical Analysis

The statistical analysis of data was carried out using GraphPad Prism® software (La Jolla, CA, USA). A student's *t*-test was carried out, in which  $p < 0.05$  (\*) was considered to indicate levels of statistical significance. All data are presented as Mean ± SE. Each experiment was repeated at least three times.

## 3. Results

### 3.1. Morphology, Cell Growth and Apoptosis of Cell Clusters of Ovarian Cancer Cell Lines

As shown in Figure 1A, 2D cell monolayers of OVCAR-5 and OVCAR-4 showed compact cell colonies, and these cells formed small clusters when cultured in a non-adherent condition. SKOV-3 grew as a loose colony pattern in cell monolayers, but formed compact cell aggregates in a non-adherent condition.

Next, the activity of two inhibitors, the EGFR inhibitor gefitinib and the dual EGFR/HER-2 inhibitor canertinib, was investigated on cell clusters of these three cell lines. The graphs in Figure 1B show that the anti-growth activity of gefitinib and canertinib was cell line-dependent. Gefitinib and canertinib significantly ( $p < 0.05$ ) reduced cell growth in OVCAR-5 clusters in a similar manner. Both the inhibitors significantly ( $p < 0.05$ ) reduced cell growth in SKOV-3 cell aggregates. However, canertinib showed ( $p < 0.05$ ) a greater decrease in growth in SKOV-3 than gefitinib. Both inhibitors had limited decrease in cell growth in OVCAR-4 clusters.

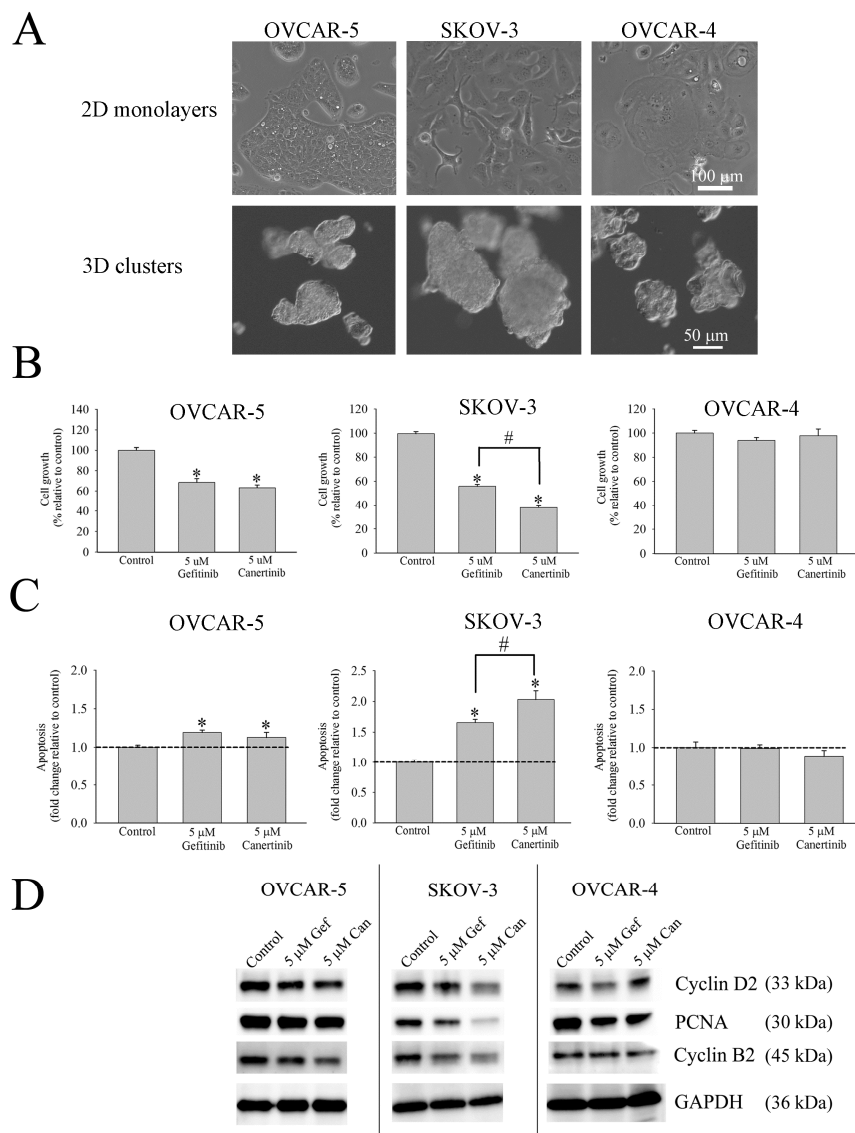


**Figure 1.** Effects of gefitinib and canertinib on three well established ovarian cancer cell lines cultured in 3D aggregates. Morphological appearances of OVCAR-5, SKOV-3, and OVCAR-4 are distinctive in monolayer. In 3D culture, both OVCAR-5 and OVCAR-4 form small clusters, but SKOV-3 cells form compact cell aggregates (A). Gefitinib and canertinib significantly reduce cell growth of OVCAR-5 cell clusters and SKOV-3 cell aggregates. OVCAR-4 cells do not show any growth response to inhibitors (B). Canertinib induces greater apoptotic cells in SKOV-3 cell aggregates than gefitinib (C). Proteins associated with the cell cycle, cyclin D2, PCNA, and cyclin B2, are reduced in SKOV-3 canertinib treated cell aggregates (D). Number of cells in control and treatment arms in Figure 1B were obtained by counting cells with a haemocytometer. Apoptotic cells were detected by Annexin V-FITC labelling cells and analysed with a flow cytometry. Representative analysis from a set of four independent experiments (Mean  $\pm$  SE;  $n = 4$ ) is presented and statistical significance was determined by a *t*-test (\*,  $p < 0.05$ ).

The decrease in cell growth by both inhibitors may be attributed to the increase of apoptosis. As shown in Figure 1C, both gefitinib and canertinib marginally ( $p < 0.05$ ) increased apoptotic cells in OVCAR-5 cell clusters. However, there was a more prominent increase of cell apoptosis of SKOV-3 aggregates treated with canertinib, than those treated with gefitinib ( $p < 0.05$ ). OVCAR-4 did not have significantly increased apoptotic cells. As shown in Figure 1D, canertinib reduced the expression of cyclin D2, PCNA and cyclin B2 in SKOV-3 cell aggregates. However, gefitinib had a limited effect

on the decrease in these proteins. OVCAR-5 and OVCAR-4 cell clusters did not change the level of these proteins with either gefitinib or canertinib treatment. These results suggest that the response to gefitinib and canertinib is cell line dependent.

### 3.2. Responsiveness of Ovarian Cancer Cell Line to Gefitinib and Canertinib Is Receptor Dependent

The cells response to both inhibitors may be due to the presence of EGFR and HER-2 proteins. We and others have previously reported that the SKOV-3 cell line has a high expression of EGFR and HER-2 [18,19,22]. In this study, only canertinib significantly reduced the total expression of EGFR (Figure 2A;  $p < 0.05$ ), p-EGFR (Figure 2B;  $p < 0.05$ ), HER-2 (Figure 2C;  $p < 0.05$ ) and p-HER-2 (Figure 2D;  $p < 0.05$ ). In addition, only canertinib significantly reduced p-AKT (Figure 2F;  $p < 0.05$ ), but p-ERK showed a tendency to decrease which was not significant (Figure 2H;  $p = 0.1320$ ). Canertinib did not alter the levels of expression or phosphorylation of these proteins in OVCAR-5 and OVCAR-4 cell clusters (data not shown). These results may suggest that the positive response to canertinib may be associated with the protein level of EGFR and HER-2 expression.

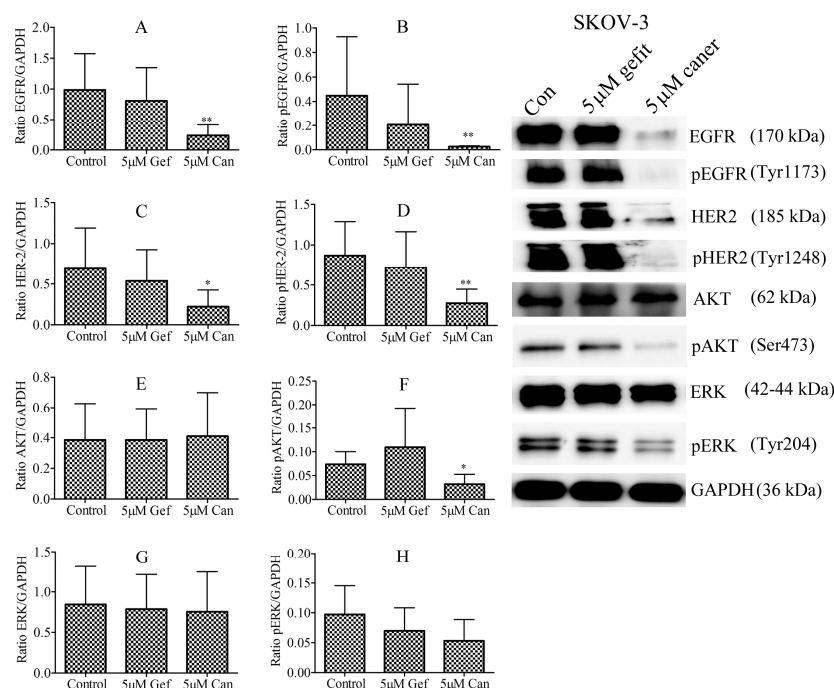


**Figure 2.** The effect of gefitinib and canertinib on the total protein level and phosphorylation of EGFR, HER-2, AKT, and ERK in SKOV-3 cell aggregates, as shown by densitometry and Western blot. Canertinib, but not gefitinib, significantly reduced both EGFR (A), pEGFR (B), HER-2 (C), and pHER-2 (D). Total expression of AKT was not changed by both inhibitors (E). Only canertinib significantly reduced pAKT (F). The levels ERK and pERK do not significantly change in any treatment (G,H). Representative analysis from a set of five independent experiments (Mean  $\pm$  SE;  $n = 5$ ) is presented, and statistical significance was determined by a *t*-test (\*,  $p < 0.05$ , \*\*,  $p < 0.01$ ).

### 3.3. Characterisation of Cells from Ascitic Fluids

We next investigated whether cells derived from the ascitic fluid of advanced ovarian cancer patients might respond to gefitinib and canertinib in a similar manner to the well-established ovarian cancer cell lines. We collected ascitic fluids from 20 patients. Table 1 represents the clinical information of 20 patients in this study. The median age of patients was 65 years (range 50–81 years old), and 13 (65%) patients were stage IIIC. Of 20 patients, 19 (95%) had high-grade serous ovarian cancer, and 12 (60%) were newly diagnosed with ascitic fluid build-up without having received any chemotherapy.

Five (25%) patients had previously received Taxol/carboplatin treatment prior to the collection of ascitic fluids. Three (15%) patients were previously treated with Taxol/carboplatin/gemcitabine.

**Table 1.** Clinical characteristics of 20 ovarian cancer patients from a gynaecological ward, Christchurch’s Women Hospital, Christchurch, New Zealand. Of 20 patients, 19 were high grade serous (HGS) subtypes and one was a low grade serous (LGS) subtype. At the time of collecting ascitic fluids, 12 patients were newly diagnosed without having received any chemotherapy (N-C). Four patients displayed carboplatin-paclitaxel (Car/Pac) resistant tumours. One patient was carboplatin-taxol (Car/Taxol) resistant. Three patients displayed carboplatin-paclitaxel-gemcitabine (Car/Pac/Gem) resistant tumours.

Patient ID	Ages	Subtypes	Stages	Treatment
1	59	HGS	IIIC	Car/Pac
2	74	HGS	IIC	N-C
3	70	HGS	IIIC	Car/Pac
4	67	HGS	IV	Car/Pac/Gem
5	74	HGS	IIIC	N-C
6	73	HGS	IIIC	N-C
7	50	HGS	IV	N-C
8	75	LGS	IIC	N-C
9	61	HGS	IIIC	N-C
10	58	HGS	IIIA	N-C
11	74	HGS	IIC	Car/Pac/Gem
12	50	HGS	IIIC	N-C
13	81	HGS	IIIC	Car/Pac/Gem
14	59	HGS	IIIC	Car/Pac
15	63	HGS	IIIC	Car/Pac
16	53	HGS	IIIC	N-C
17	56	HGS	IIIC	Car/Taxol
18	59	HGS	IC	N-C
19	67	HGS	IIIC	N-C
20	67	HGS	IIIC	N-C

#### 3.4. Identification of EGFR and HER-2 in Cells Isolated from Ascitic Fluid

To identify whether cells from ascitic fluid were epithelial in origin, we used an array of well-known protein markers, previously described in the association with ovarian cancer cell lines. Before investigating the protein markers in ascitic fluid-derived cells, we tested the specificity of the antibodies for selective proteins of interest in two well established ovarian cancer cell lines (Figure 3). Figure 3A demonstrates the immunological specificity of anti-EGFR and anti-HER-2 antibodies in ovarian cancer cell lines. OVCAR-5 showed a high level of EGFR, but a low level of HER-2 proteins. The SKOV-3 cell line showed a highly positive expression of both EGFR and HER-2. We next used this protocol to determine the expression of these two proteins in ascitic fluid-derived cells. Figure 3B demonstrates the three different staining patterns that we categorise based on the staining of EGFR and HER-2. Low expression was depicted by a lack of plasma membrane staining. Moderate expression showed some plasma membrane-associated receptors, and high expression had strong plasma membrane-associated receptor staining (Figure 3B).

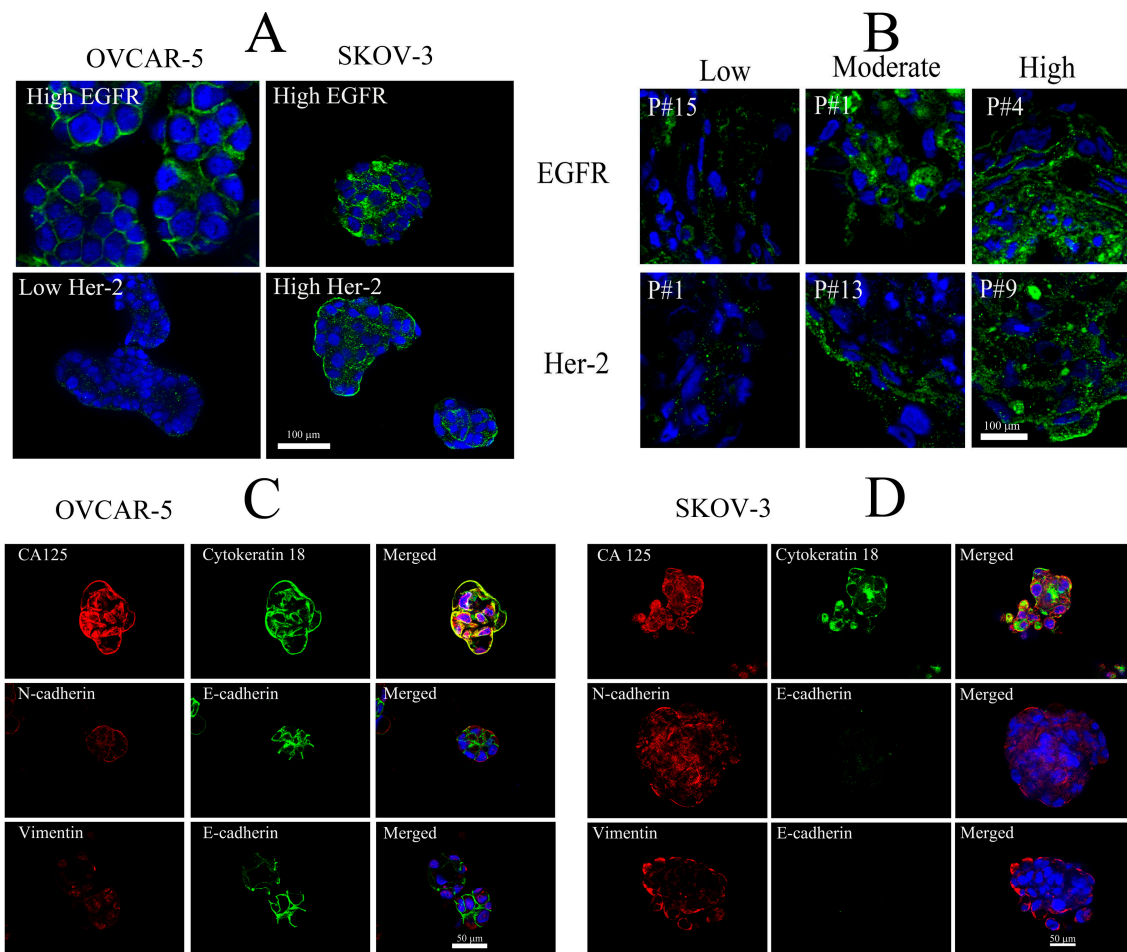


**Figure 3.** The expression of selected protein markers in ovarian cancer cell lines, OVCAR-5 and SKOV-3, and ascitic fluid derived cells. OVCAR-5 shows a membrane positive staining for EGFR and negative staining for HER-2. SKOV-3 cell aggregates show membrane positive expression of EGFR and HER-2 (A). Ascitic fluid-derived cells show positive immunostaining for EGFR and HER-2 (B). OVCAR-5 shows positive staining for CA125, cytokeratin-18 and E-cadherin, but low expression of mesenchymal protein markers, N-cadherin and vimentin (C). SKOV-3 cell aggregates are positive for the staining of CA125, cytokeratin-18, N-cadherin, and vimentin, but very low for E-cadherin (D).

### 3.5. Immunostaining of Selective Protein Markers for Ovarian Cancer

We also documented protein markers that were previously known to be found in ovarian cancer cells. These proteins were CA125, cytokeratin-18, E-cadherin, N-cadherin and vimentin. Again, we confirmed the immunological specificity using OVCAR-5 and SKOV-3, before using these antibodies with ascitic fluid-derived cells.

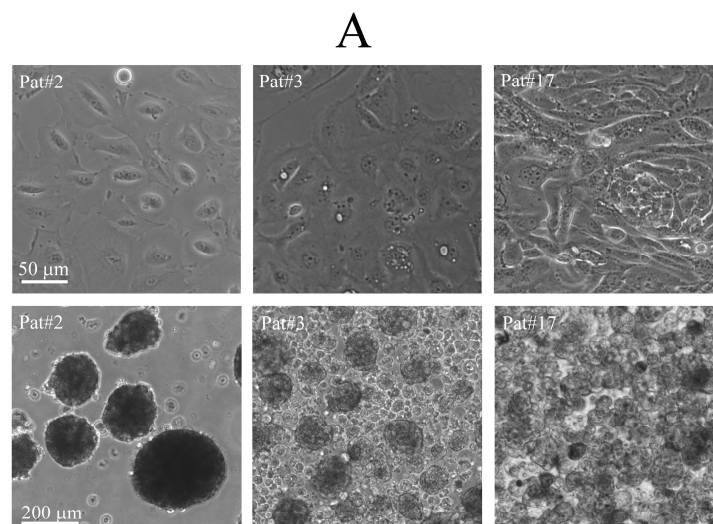
The immunostaining for CA125, cytokeratin-18, E-cadherin and N-cadherin was positively observed in the OVCAR-5 cell lines. However, vimentin was less prominent in this cell line (Figure 3C). In contrast, the SKOV-3 cell line showed positive immunostaining of N-cadherin, vimentin, CA-125 and cytokeratin-18. There was a low but detectable level of E-cadherin expression in this cell line (Figure 3D).

Table 2 and Figure 4 summarise all relevant characteristics of ascitic fluid-derived cell samples. In Table 2, four of the 20 samples formed compact colonies and 16 showed loose colonies when they were cultured in cell monolayers. When cultured in a non-adherent condition, 12 (60%) of the samples formed compact aggregates, 7 (35%) of the samples showed small clusters, and 1 (5%) had a single-cell appearance.

**Table 2.** Summary of characteristics of ascitic fluid-derived cells that are cultured in in vitro condition and selective protein markers for epithelial cells.

Characteristic	Number	(%)
<b>Ovarian cancer Patients</b>	20	
<b>Cell morphology</b>		
<b>Cell monolayer</b>		
Compact colony	4	20
Loose colony	16	80
<b>Floating condition</b>		
Compact aggregates	12	60
Small cluster	7	35
Single cells	1	5
<b>Protein expression</b>		
CA125	20	100
Cytokeratin-18	19	95
E-cadherin	5	25
N-cadherin	20	100
Vimentin	19	95
High EGFR only	9	45
High HER-2 only	0	
High EGFR/HER-2	8	40
Low EGFR/HER-2	3	15

Figure 4A,B show the characteristics of growth patterns in cell monolayers and non-adherent culture conditions and the immunostaining of selective proteins in selective ascitic-derived cell samples. In the Table 2, nine (45%) of the 20 patient cells showed a detectable level of EGFR. Eight (40%) showed both expression of EGFR and HER-2 in the same cells. Three (15%) showed a low but detectable expression of EGFR and HER-2. There was no detection of HER-2 alone in any patient cells. Five (25%) of the 20 showed E-cadherin staining associated with the plasma membrane. All were positive for CA-125 and N-cadherin, whilst 19 (95%) expressed vimentin and cytokeratin-18.



**Figure 4.** Cont.

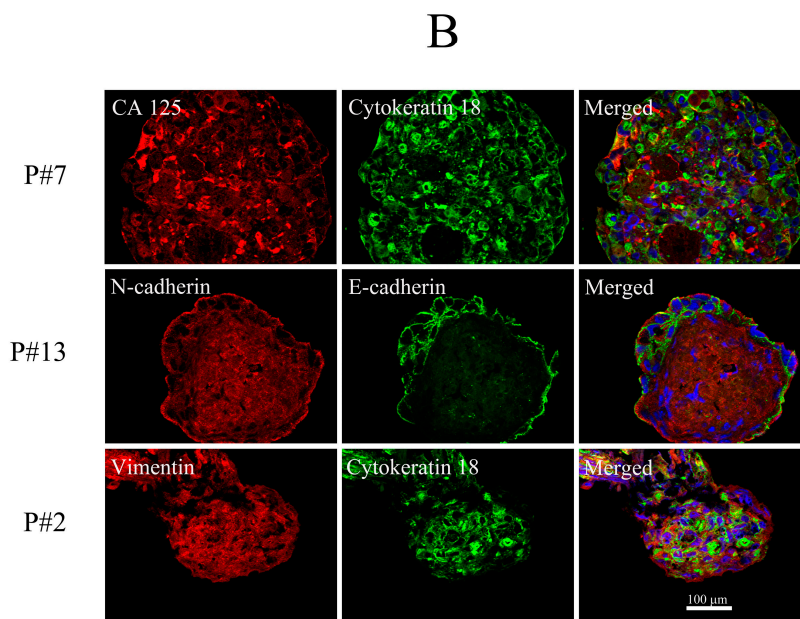


**Figure 4.** Morphological appearances of ascitic fluid-derived cells from selected patients are cultured in a cell monolayer and a 3D cell suspension. Cells cultured in the 3D cell suspension display three distinct patterns consisting of compacted spheroids, small clusters and loose single cells (A). Ascitic fluid derived cells from selected patients cultured in a 3D cell suspension positively express CA125, cytokeratin-18, N-cadherin, E-cadherin and vimentin (B).

### 3.6. Effects of Gefitinib and Canertinib on Cellular Viability Using Alamar Blue Dye Assay

To study the effect of gefitinib and canertinib on the cell viability of EGFR and HER-2 positive ascitic-derived cells, we examined the cellular conversion of the Alamar blue dye, which was converted by cells from blue into pink colour, as an indirect predictor of cell viability. As shown in Table 3A, gefitinib and canertinib selectively reduced viability in the EGFR positive ascitic cells. Of nine ascitic cell samples, four gefitinib-treated ascitic cell samples (patient numbers 1, 4, 17, 19;  $p < 0.05$ ) had lower viability than the control cells. Four canertinib-treated cells (patient numbers 4, 6, 17, 19;  $p < 0.05$ ) also showed a reduction in cellular viability compared to the control cells. Both gefitinib and canertinib reduced viability in three patient cells (patient numbers 4, 17, 19). Canertinib ( $74.9\% \pm 4.3\%$ ,  $p < 0.05$ ) reduced viability to a greater degree than gefitinib ( $84.6 \pm 0.8$ ) in patient number 4.

Table 3B shows that ascitic cells expressing both EGFR and HER-2 did not reduce cellular viability after exposure to gefitinib. However, three out of eight EGFR and HER-2 positive ascitic cell samples (patient numbers 9, 11, 16;  $p < 0.05$ ) treated with canertinib had lower cellular viability than the control cells. Similarly, the EGFR and HER-2 positive cell line SKOV-3, used as an internal control cell line, showed a decrease in cellular viability only with canertinib treatment (Table 3B;  $p < 0.05$ ). These results may suggest that a dual inhibition of EGFR and HER-2 with canertinib may be a better option than gefitinib to inhibit ovarian cancer cells in ascitic fluids that are EGFR and HER-2 positive. Out of three low EGFR and HER-2 expressing cells, only patient number 2 showed reduced cellular viability by both gefitinib and canertinib (Table 3C;  $p < 0.05$ ).

**Table 3.** Cellular viability of OVCAR-5, SKOV-3 and ascitic derived cells from 20 patients are affected by gefitinib (Gef) and canertinib (Can). Nine patient cell lines and the OVCAR-5 cells expressing EGFR only, have a decrease in viability by the treatment of Gef and Can (A). Eight patient cell lines and SKOV-3 cells expressing both EGFR and HER-2 do not respond to Gef, but have increased responsiveness to Can (B). Only one cell sample of EGFR/HER-2 negative cells responded to both gefitinib and canertinib (C). Representative analysis was from a set of two independent experiments, and each experiment had three duplicates. Mean  $\pm$  SE;  $n = 2$  is presented and statistical significance was determined by a *t*-test (\*,  $p < 0.05$ ). The statistical difference between gefitinib and canertinib treated cells was determined by a *t*-test (#,  $p < 0.05$ ).

(A) (+) EGFR			
Patient ID	Control	Cellular Viability (Relative to Control %)	
		5 $\mu$ M Gef	5 $\mu$ M Can
OVCAR-5	100	99.9 $\pm$ 1.3	102 $\pm$ 1.2
1	100	74.6 $\pm$ 2.7 *	87.8 $\pm$ 17.6
3	100	98.9 $\pm$ 6.7	104.5 $\pm$ 4.6
4	100	84.6 $\pm$ 0.8 *	74.9 $\pm$ 4.3 *#
6	100	95.5 $\pm$ 3.1	91.7 $\pm$ 1.9 *
8	100	93.6 $\pm$ 3.1	92.5 $\pm$ 3.9
10	100	102.8 $\pm$ 5.5	95.4 $\pm$ 2.7
17	100	86.3 $\pm$ 1.1 *	89.8 $\pm$ 1.3 *
19	100	86.9 $\pm$ 2.0 *	78.4 $\pm$ 4.1 *
20	100	102.8 $\pm$ 5.5	95.4 $\pm$ 2.7
(B) (+) EGFR/HER-2			
Patient ID	Control	Cellular Viability (Relative to Control %)	
		5 $\mu$ M Gef	5 $\mu$ M Can
SKOV-3	100	95.2 $\pm$ 2.7	82.9 $\pm$ 2.8 *
7	100	105.1 $\pm$ 2.1	117.1 $\pm$ 4.5
9	100	91.7 $\pm$ 30	81.4 $\pm$ 33.3 *
11	100	87.8 $\pm$ 6.5	82.8 $\pm$ 7.4 *
12	100	86.5 $\pm$ 6.8	90.3 $\pm$ 4.6
13	100	94.3 $\pm$ 4.4	92.7 $\pm$ 4.3
15	100	95.4 $\pm$ 3.1	93.9 $\pm$ 2.1
16	100	95.6 $\pm$ 6.2	88.2 $\pm$ 1.9 *
18	100	99.8 $\pm$ 4.9	102.7 $\pm$ 2.5
(C) (-) EGFR/HER-2			
Patient ID	Control	Cellular Viability (Relative to Control %)	
		5 $\mu$ M Gef	5 $\mu$ M Can
2	100	68.3 $\pm$ 0.11 *	65.3 $\pm$ 11.2 *
5	100	95.3 $\pm$ 0.58	97.6 $\pm$ 0.78
14	100	96.45 $\pm$ 1.4	96.56 $\pm$ 0.12

### 3.7. Effect of Gefitinib and Canertinib on Total Expression and Activation of EGFR and HER-2 Proteins

We further evaluated the effect of gefitinib and canertinib on the protein level of EGFR and HER-2 and their associated phosphorylation at tyrosine 1173 and tyrosine 1248 residues, respectively in ascitic fluid-derived cell samples. As shown in Table 4A, in the EGFR positive cells, five out of nine samples (patient numbers 1, 4, 6, 10, 20;  $p < 0.05$ ) showed a decrease in EGFR expression after gefitinib treatment. The phosphorylation of EGFR was also compromised by gefitinib. Six out of nine ascitic cell samples (patient numbers 1, 3, 6, 10, 17, 20;  $p < 0.05$ ) showed a decrease in the phosphorylation of EGFR after gefitinib treatment. Also, canertinib reduced the level of EGFR and pEGFR. Canertinib reduced the total expression of EGFR in five out of nine cells samples (patient numbers 1, 3, 4, 6, 20;  $p < 0.05$ ) and pEGFR in five samples (patient numbers 1, 3, 4, 17, 20;  $p < 0.05$ ).

**Table 4.** The protein level and phosphorylation of EGFR and HER-2 in ascitic fluid derived cells that are exposed to gefitinib (Gef) and canertinib (Can). Gef and Can demonstrate the selective decrease in EGFR and pEGFR in ascitic fluid EGFR positive cells (A). Similarly, ascitic fluid derived cells with EGFR/HER-2 positive cells respond to Gef and Can randomly reduce EGFR, pEGFR, HER-2 and pHER-2 (B,C). Expressions of EGFR, pEGFR, HER-2 and pHER-2 were obtained from the fluorescent intensity of immunofluorescent staining of corresponding proteins. The fluorescent intensity was calculated from at least five cell clusters and aggregates from cells that were prepared by frozen sections. The fluorescent intensity of the control is normalised to 100 percent and the fluorescent intensity of treatment is calculated relatively to the control sample. Representative analysis is presented from a set of two independent experiments; each experiment had at least three duplicates (Mean  $\pm$  SE;  $n = 2$ ) and statistical significance was determined by a *t*-test (\*,  $p < 0.05$ ).

(A) (+) EGFR					
Patient ID	Control	EGFR (% Relative Expression to Control)		pEGFR (% Relative Expression to Control)	
		5 $\mu$ M Gef	5 $\mu$ M Can	5 $\mu$ M Gef	5 $\mu$ M Can
1	100	65.93 $\pm$ 6.6 *	72.59 $\pm$ 1.5 *	76.04 $\pm$ 3.2 *	67.36 $\pm$ 3.0 *
3	100	86.51 $\pm$ 4.3	58.8 $\pm$ 10.4 *	82.31 $\pm$ 4.37 *	68.25 $\pm$ 3.6 *
4	100	47.82 $\pm$ 4.3 *	32.85 $\pm$ 3.9 *	83.97 $\pm$ 6.2	54.52 $\pm$ 2.8 *
6	100	71.55 $\pm$ 3.9 *	60.25 $\pm$ 2.4 *	69.27 $\pm$ 6.8 *	85.94 $\pm$ 4.2
8	100	144.8 $\pm$ 5.9	108.3 $\pm$ 6.9	98.97 $\pm$ 2.8	84.83 $\pm$ 2.8
10	100	57.64 $\pm$ 2.5 *	97.92 $\pm$ 4.6	61.19 $\pm$ 5.9 *	131.43 $\pm$ 4.3
17	100	83.99 $\pm$ 18.3	124.1 $\pm$ 5.3	66.37 $\pm$ 2.7 *	68.51 $\pm$ 2.1 *
19	100	122.3 $\pm$ 6.9	142.2 $\pm$ 5.5	99.18 $\pm$ 2.5	111 $\pm$ 6.7
20	100	72.68 $\pm$ 9.8 *	79.63 $\pm$ 4.1 *	73.53 $\pm$ 2.5 *	75.8 $\pm$ 3.7 *
(B) (+) EGFR/HER-2					
Patient ID	Control	EGFR (% Relative Expression to Control)		pEGFR (% Relative Expression to Control)	
		5 $\mu$ M Gef	5 $\mu$ M Can	5 $\mu$ M Gef	5 $\mu$ M Can
7	100	141.2 $\pm$ 10.5	132.4 $\pm$ 8.14	145.1 $\pm$ 13.7	74.63 $\pm$ 5.9 *
9	100	62.4 $\pm$ 10.87 *	52.2 $\pm$ 6.58 *	69.6 $\pm$ 2.1 *	72.4 $\pm$ 12.2 *
11	100	87.3 $\pm$ 5.5	66.9 $\pm$ 3.8 *	86.3 $\pm$ 9.1	77.7 $\pm$ 2.0 *
12	100	75.3 $\pm$ 5.4	62.4 $\pm$ 2.2 *	126.4 $\pm$ 6.3	116.1 $\pm$ 5.5
13	100	66.5 $\pm$ 5.4 *	67.3 $\pm$ 4.6 *	93.6 $\pm$ 3.5	92.1 $\pm$ 3.6
15	100	83.4 $\pm$ 8.6	93.3 $\pm$ 5.6	90.7 $\pm$ 2.6	78.4 $\pm$ 2.7
16	100	96.1 $\pm$ 7.1	119.8 $\pm$ 9.5	84.3 $\pm$ 1.7	91 $\pm$ 4.4
18	100	74.3 $\pm$ 8.1	66.0 $\pm$ 6.9 *	91.5 $\pm$ 2.4	95.9 $\pm$ 4.6
(C) (+) EGFR/HER-2					
Patient ID	Control	Her-2 (% Relative Expression to Control)		pHer-2 (% Relative Expression to Control)	
		5 $\mu$ M Gef	5 $\mu$ M Can	5 $\mu$ M Gef	5 $\mu$ M Can
7	100	100.3 $\pm$ 11.4	123.4 $\pm$ 9.5	78.7 $\pm$ 3.7	95.0 $\pm$ 8.3
9	100	106.2 $\pm$ 6.12	64.6 $\pm$ 1.3 *	110 $\pm$ 6.11	62.5 $\pm$ 6.1 *
11	100	115.7 $\pm$ 7.2	81.9 $\pm$ 7.1	87.3 $\pm$ 5.7	92.3 $\pm$ 6.3
12	100	128.7 $\pm$ 6.3	128.8 $\pm$ 2.3	117.6 $\pm$ 6.7	107.8 $\pm$ 3
13	100	78.9 $\pm$ 5.2	99 $\pm$ 8.4	94.7 $\pm$ 7.4	114.6 $\pm$ 4.4
15	100	86.2 $\pm$ 5.6	62.8 $\pm$ 3.1 *	104.1 $\pm$ 7.6	77.6 $\pm$ 2.5 *
16	100	78.5 $\pm$ 2.3	103.8 $\pm$ 3.5	100.8 $\pm$ 7.6	109.4 $\pm$ 5.2
18	100	72.22 $\pm$ 9.4	43.7 $\pm$ 6.3 *	115.8 $\pm$ 3.7	100.8 $\pm$ 7.2

The level of protein and phosphorylation of EGFR and HER-2 expressing cells is shown in Table 4B,C. Only two out of eight ascitic fluid-derived cell samples (patient numbers 9 and 13;  $p < 0.05$ ) had reduced expression of EGFR by gefitinib. However, five out of eight cell samples (patient numbers 9, 11, 12, 13, 18;  $p < 0.05$ ) showed the decrease in EGFR expression with canertinib treatment. Only one (patient number 9;  $p < 0.05$ ) and three (patient numbers 7, 9, 11;  $p < 0.05$ ) had reduced pEGFR by gefitinib or canertinib, respectively. We also evaluated the protein and phosphorylation of HER-2 in the EGFR and HER-2 positive ascitic cells (Table 4C). Only canertinib reduced the expression of

HER-2 in three patient cell samples (patient numbers 9, 15, 18;  $p < 0.05$ ) and pHER-2 in two patient cell samples (patient numbers 9 and 15;  $p < 0.05$ ).

### 3.8. Effect of Gefitinib and Canertinib on PCNA, Caspase-3, pERK and pAKT

To better understand the effect of gefitinib and canertinib on signalling proteins that are commonly known with the activation of EGFR and HER-2, we investigated the immunostaining of PCNA, cleaved caspase-3, pERK and pAKT. As shown in Table 5A,B, of eight ascitic cell samples, gefitinib reduced the PCNA in two samples (patient numbers 3 and 20;  $p < 0.05$ ) in EGFR positive cells. Similarly, canertinib also reduced PCNA in two samples (patient numbers 19 and 20;  $p < 0.05$ ). Two ascitic cell samples (patient numbers 10 and 20;  $p < 0.05$ ) increased cleaved caspase-3 protein expression after gefitinib treatment. Only cells from patient number 10 increased cleaved caspase-3 after exposure to canertinib. The phosphorylation of ERK (Tyr 204) and AKT (Ser 473) was randomly and broadly affected. As shown in Table 5B, gefitinib reduced pERK in four ascitic cell samples (patient numbers 3, 4, 19, 20;  $p < 0.05$ ). Canertinib reduced pERK in five samples (patient numbers 4, 6, 8, 19, 20;  $p < 0.05$ ). Gefitinib reduced pAKT in five cell samples (patient numbers 4, 6, 10, 19, 20;  $p < 0.05$ ). Canertinib reduced pAKT in four cell samples (patient numbers 4, 8, 19, 20;  $p < 0.05$ ).

**Table 5.** The protein level of PCNA, cleaved caspase-3, pERK (Tyr 204) and pAKT (Ser 473) in EGFR positive cells are affected by gefitinib (Gef) and canertinib (Can). The changes of PCNA and cleaved caspase-3 in Gef and Can treated cells are not prominent (A). The decrease in pERK (Tyr 204) and pAKT (Ser 473) is random in some selected patient cells (B). The fluorescent intensity of control is normalised to 100% and the fluorescent intensity of treatment is calculated relatively to the control sample. Representative analysis was from a set of two independent experiments and each experiment had at least three duplicates. Mean  $\pm$  SE;  $n = 2$  is presented and statistical significance was determined by a *t*-test (\*,  $p < 0.05$ ).

(A) EGFR positive cells					
Patient ID	Control	PCNA (% Relative Expression to Control)		Cleaved Caspase-3 (% Relative Expression to Control)	
		5 $\mu$ M Gef	5 $\mu$ M Can	5 $\mu$ M Gef	5 $\mu$ M Can
3	100	81.8 $\pm$ 5.1 *	90.7 $\pm$ 3.3	73.7 $\pm$ 3.6	88.0 $\pm$ 6.2
4	100	100 $\pm$ 7.2	88.5 $\pm$ 5.2	96.3 $\pm$ 11.7	81.4 $\pm$ 7.7
6	100	93.4 $\pm$ 4.1	87.7 $\pm$ 2.3	91.2 $\pm$ 6.3	88.9 $\pm$ 3.2
8	100	108.9 $\pm$ 6.2	121.4 $\pm$ 3.2	90.0 $\pm$ 3.7	100 $\pm$ 2.1
10	100	93.9 $\pm$ 3.12	99.2 $\pm$ 3.6	300 $\pm$ 32 *	357.7 $\pm$ 37.2 *
17	100	84.6 $\pm$ 3.1	90.5 $\pm$ 3.8	83.7 $\pm$ 2.8	76.4 $\pm$ 2.7
19	100	119.5 $\pm$ 3.8	62.8 $\pm$ 4.8 *	130.4 $\pm$ 27	54.6 $\pm$ 4.5
20	100	63.6 $\pm$ 3.0 *	56.7 $\pm$ 4.3 *	165.7 $\pm$ 11.9 *	128.9 $\pm$ 14.2

(B)					
Patient ID	Control	pErk (% Relative Expression to Control)		pAkt (% Relative Expression to Control)	
		5 $\mu$ M Gef	5 $\mu$ M Can	5 $\mu$ M Gef	5 $\mu$ M Can
3	100	86.9 $\pm$ 4 *	116.4 $\pm$ 5.3	101.6 $\pm$ 4.3	111.2 $\pm$ 3.5
4	100	65.2 $\pm$ 2.2 *	67.4 $\pm$ 3.7 *	46.2 $\pm$ 5.0 *	50.6 $\pm$ 6.4 *
6	100	95.7 $\pm$ 4.6	77.8 $\pm$ 2.6 *	88.4 $\pm$ 2.6 *	90.1 $\pm$ 5.3
8	100	120.6 $\pm$ 3.4	79.7 $\pm$ 3.4 *	95.6 $\pm$ 2.3	73.2 $\pm$ 3.8 *
10	100	96.6 $\pm$ 3.7	104.7 $\pm$ 2.3	70.9 $\pm$ 7.8 *	92.0 $\pm$ 3.8
17	100	96.4 $\pm$ 3.0	94.3 $\pm$ 5.6	81 $\pm$ 3.8	103.4 $\pm$ 7.2
19	100	65.2 $\pm$ 1.5 *	58.6 $\pm$ 1.3 *	82.1 $\pm$ 2.1 *	76.9 $\pm$ 2.4 *
20	100	62.1 $\pm$ 3.2 *	49.4 $\pm$ 2.9*	82.5 $\pm$ 2.6 *	68.9 $\pm$ 3.5 *

With the EGFR and HER-2 positive ascitic cells as shown in Table 6A,B, both gefitinib and canertinib showed a limited decrease in PCNA and an increase in cleaved caspase-3. Only one patient cell sample (patient number 9;  $p < 0.05$ ) showed reduced PCNA after gefitinib treatment. Both gefitinib and canertinib induced cleaved caspase-3 only in one patient cell sample (patient number 7;  $p < 0.05$ ). Table 6B shows the effect of gefitinib and canertinib on the phosphorylation of ERK (Tyr 204) and AKT (Ser 473). Canertinib showed a greater decrease in pERK (Tyr 204) in five ascitic cell samples (patient numbers 7, 9, 11, 13, 16;  $p < 0.05$ ) than gefitinib, which affected only one cell sample (patient number 16;  $p < 0.05$ ). The decrease in pAKT (Ser 473) was less prominent, but canertinib still reduced pAKT (Ser 473) in four patient cell samples (patient numbers 7, 9, 11, 13;  $p < 0.05$ ), which was greater than gefitinib, which reduced pAKT (Ser 473) in only one patient cell sample (patient number 13;  $p < 0.05$ ).

**Table 6.** The expressions of PCNA, cleaved caspase-3, pERK (Tyr 204) and pAKT (Ser 473) in EGFR/HER-2 positive cells are affected by gefitinib (Gef) and canertinib (Can). The changes of PCNA and cleaved caspase-3 in Gef and Can treated cells are limited (A). The decreases in pERK (Tyr 204) and pAKT (Ser 473) are more evident on Can than Gef treated cell samples (B). The fluorescent intensity of the control is normalised to 100% and the fluorescent intensity of treatment is calculated relative to the control sample. Representative analysis is presented from a set of two independent experiments and each experiment had at least three duplicates (mean  $\pm$  SE;  $n = 2$ ). Statistical significance was determined by a *t*-test (\*,  $p < 0.05$ ).

(A) EGFR/HER-2 positive cells					
Patient ID	Control	PCNA (% Relative Expression to Control)		Cleaved Caspase-3 (% Relative Expression to Control)	
		5 $\mu$ M Gef	5 $\mu$ M Can	5 $\mu$ M Gef	5 $\mu$ M Can
7	100	117.7 $\pm$ 5	187.9 $\pm$ 20.2	346.9 $\pm$ 37.4 *	426.3 $\pm$ 17.8 *
9	100	63.2 $\pm$ 4.2 *	77.6 $\pm$ 11.6	98.5 $\pm$ 16.7	121.5 $\pm$ 17.8
11	100	84.2 $\pm$ 8.4	87.1 $\pm$ 4.8	86 $\pm$ 8.4	75.1 $\pm$ 3.6
12	100	116.3 $\pm$ 4.37	123.7 $\pm$ 6.23	89.1 $\pm$ 2.67	79.7 $\pm$ 2.66
13	100	137 $\pm$ 5.2	101 $\pm$ 4.1	113.3 $\pm$ 3.2 *	117.6 $\pm$ 9.4
15	100	92.8 $\pm$ 2.7	120.6 $\pm$ 6.6	97.6 $\pm$ 5.2	92.6 $\pm$ 2.8
16	100	83.7 $\pm$ 6.9	87.9 $\pm$ 4.5	76.8 $\pm$ 3.2	92.3 $\pm$ 2.9
18	100	113.2 $\pm$ 10.4	99.5 $\pm$ 4.9	94.3 $\pm$ 4.9	93 $\pm$ 4.4

(B)					
Patient ID	Control	pErk (% Relative Expression to Control)		pAkt (% Relative Expression to Control)	
		5 $\mu$ M Gef	5 $\mu$ M Can	5 $\mu$ M Gef	5 $\mu$ M Can
7	100	99.4 $\pm$ 3.6	70.5 $\pm$ 4.9 *	104 $\pm$ 4.1	75.3 $\pm$ 4.8 *
9	100	138.5 $\pm$ 10.9	65.43 $\pm$ 3.4 *	120.4 $\pm$ 12.95	69.5 $\pm$ 4.3 *
11	100	93.2 $\pm$ 3.9	84.3 $\pm$ 2.9 *	96.4 $\pm$ 7.1	83.6 $\pm$ 3.1 *
12	100	95.1 $\pm$ 5.3	88.9 $\pm$ 5.4	119.3 $\pm$ 12.8	87.8 $\pm$ 4
13	100	89.8 $\pm$ 5.3	57.4 $\pm$ 1.3 *	76.9 $\pm$ 3.1 *	55.4 $\pm$ 1.9 *
15	100	120.4 $\pm$ 3.9	104.4 $\pm$ 3.7	95.3 $\pm$ 3.6	92.6 $\pm$ 2.7
16	100	78.3 $\pm$ 4.7 *	80.1 $\pm$ 2.3 *	106 $\pm$ 4.5	96.3 $\pm$ 3.6
18	100	196.5 $\pm$ 9.7	157.5 $\pm$ 17.2	127.2 $\pm$ 2.5	115.8 $\pm$ 7.5

We next pooled all the effects caused by gefitinib and canertinib on the decrease in PCNA, EGFR, pEGFR, pAKT and pERK, the increase of cleaved caspase-3 in EGFR positive ascitic cells and the inclusion of HER-2 and pHER-2 in EGFR and HER-2 positive ascitic cells (Table 7). We then questioned whether gefitinib or canertinib was more effective in EGFR positive ascitic cells. As shown in the Table 7A, both inhibitors equally affected the EGFR positive cells. We also analysed these effects on EGFR and HER-2 positive ascitic cells (Table 7B). Interestingly, canertinib showed greater inhibition than gefitinib in EGFR and HER-2 positive cells ( $p = 0.0006$ , Fisher's exact test).

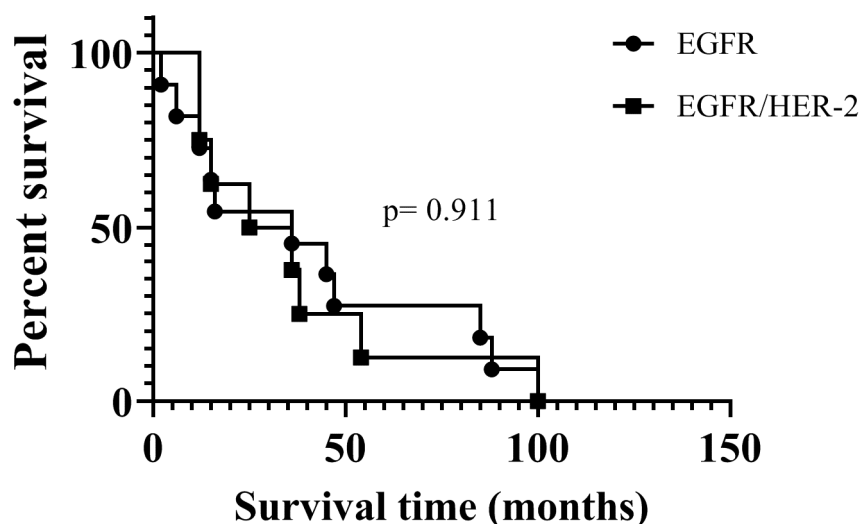
**Table 7.** Total responsiveness of EGFR and EGFR and HER-2 positive cells are compared between gefitinib and canertinib. Numbers of decrease in PCNA, EGFR, pEGFR, HER-2, pHER-2, pERK, and pAKT in EGFR positive cells (A) and EGFR and HER-2 positive cells (B) are counted, and data are subjected to statistical analysis, using Fisher's exact test.

(A) (+) EGFR		
Inhibitors	Response	No Response
Gefitinib	24	26
Canertinib	24	26

B (+) EGFR/HER-2		
Inhibitors	Response	No Response
Gefitinib	6	58
Canertinib	23	41

In addition, we evaluated clinical data to compare overall survival between women whose cells expressed EGFR, and who expressed both EGFR and HER-2. As shown in Figure 5, there is no statistical difference in the survival of patients with EGFR and EGFR/HER-2 positive cells.



**Figure 5.** Comparison of patient's survival time between ascitic fluid derived cells with positive staining for EGFR and EGFR and HER-2 proteins. There is no significant statistical difference between two groups of patients ( $p = 0.911$ ). The statistical analysis was performed by using Log-rank (Mantel-Cox) and Gehan-Breslow-Wilcoxon tests, available from a GraphPad Prism 8.0.1 version.

#### 4. Discussion

Here, we investigate the growth modulating effects of the EGFR inhibitor gefitinib and the dual EGFR and HER-2 inhibitor canertinib on three established ovarian cancer cell lines (OVCAR-5, SKOV-3 and OVCAR-4), and isolated cells from the ascitic fluid of 20 advanced ovarian cancer patients. We demonstrate that ascitic fluid-derived cells have a measurable level of EGFR and HER-2 proteins, the levels of which vary considerably among patients. The effects of gefitinib and canertinib alone on cell viability and targeted signalling molecules, (including pERK and pAKT associated with the activation of EGFR and HER-2), show variation among ascitic fluid-derived patient cells. Both gefitinib and canertinib demonstrate similar anti-tumour effects in EGFR positive cells. However, in EGFR and HER-2 positive cells, canertinib demonstrates a greater effect on the decrease in pERK and pAKT than gefitinib.

#### 4.1. Expression of Protein Markers in Ascitic Fluid-Derived Ovarian Cancer Cells

It has been recognised that metastatic lesions of advanced ovarian cancer begin with the deposition of small clusters of cancerous cells, carried around within the peritoneal cavity by the movement of ascitic fluid. The proteomic profiles of the primary tumour compared to the metastatic sites have differential patterns to some extent [10,22,23]. In addition, the proteomic signatures, associated with epithelial to mesenchymal phenotypic transition and vice versa, in ascitic fluid-derived ovarian cancer cells, have been described [24–26]. Cells derived from the ascitic fluid of ovarian cancer patients are known to express various protein markers associated with epithelial and mesenchymal phenotypes, including CD44, AC133, EGFR, integrin beta-1, cytokeratin-18 and E-cadherin [27]. Ascitic-derived cells cultured in cell monolayers and floating conditions express distinct protein markers. Adherent cells possess mesenchymal protein profiles, but floating cells display more epithelial markers [25]. Ascitic fluid cells expressing CA125 and EpCAM have been characterised in a large cohort of ovarian cancer patients [28]. Cells that have been cultured from a primary tumour and ascitic fluid display both epithelial and mesenchymal (E/M) markers. These E/M hybrid transition cells produce epithelial ovarian cancer tumours in vivo in a xenograft model [29].

In agreement with previous studies, we observe in our study that ascitic fluid-derived cells show immunostaining for CA-125, cytokeratin-18, E-cadherin, N-cadherin and vimentin. The morphological appearance of these cells, derived from ascitic fluid and cultured as a 2D cell monolayer, displays both compact colony and loose/motile characteristics. However, when these cells are cultured in a 3D cell suspension, they form three different main morphologies. The compact spheroid phenotype is displayed by the majority of ascitic cells and followed by small clusters. Evidence suggests that ovarian cancer cells have the ability to form compact spheroids, and these cells possess a myofibroblast-like phenotype, increasing invasive capacity [30]. This is consistent with our findings that the majority of ascitic-derived cells demonstrate a high expression of vimentin, a mesenchymal protein that is linked to fibroblastic phenotypes. A recently published study has demonstrated that vimentin positive cancer cells in high-grade serous tumour tissues are possibly the cells that migrate and invade the peritoneal membrane [31]. However, we apply caution to the interpretation of the protein markers that were used in our study. Even though cells in ascitic fluid were positive for epithelial cell origin, the ability of these cells to develop ovarian tumours in an animal model has not been tested. We also think that heterogeneous cells presented in ascitic fluid, including malignant and non-malignant cells, may play an important role in responsiveness to anticancer drugs.

#### 4.2. Expression of EGFR and HER-2 in Ascitic Fluid-Derived Ovarian Cancer Cells

We have also demonstrated that ascitic fluid-derived cells have measurable levels of EGFR and HER-2 protein expression. Of these samples, 45% are EGFR positive cells, 40% are EGFR/HER-2 positive and 15% have low EGFR/HER-2. However, we did not detect any cells that had HER-2 protein expression alone. Even though EGFR and HER-2 protein expression has been studied in ovarian cancer, those previous studies only identified the proteins in primary and secondary tumours, and not in cells from ascitic fluid [13,14,32]. However, a recent study has shown that both ascitic fluid-derived cells and cells from solid ovarian tumour sites have broadly expressed HER-2 protein [33]. There is a notable discrepancy of the expression levels of these proteins in these previous studies; this is perhaps due to the different technical platforms utilised to assess the protein expression. EGFR protein immuno-expression was seen in 28% of primary and 33% of corresponding recurrent ovarian serous carcinomas evaluated in a cohort of 80 patients [34]. Another study showed that primary serous ovarian cancer has varied levels of immunostained EGFR (7%), pEGFR (12%), HER-2 (5%), pAKT (8%) and pERK (37%). This study also showed a marginal increase of similar proteins in a small number of patients with recurrent disease [32]. HER-2 protein and its gene expression level are significantly higher in ovarian cancer patients, compared to patients with benign ovarian tumours and normal ovaries [14]. In a cohort of 52 patients with invasive epithelial ovarian cancer, EGFR is expressed in 59% of the cases, and HER-2 expression is found in 35%, without any mutations of the tyrosine

kinase domains of EGFR and HER-2 [35]. The study showed that of 50 patients with high-grade serous ovarian carcinomas, HER-2 was only expressed by 29%. More importantly, this study also showed that cells derived from ascitic fluid over-express HER-2 when compared to normal ovarian epithelial cells. However, the study did not use alternative protein markers to confirm whether cells derived from ascitic fluids were actually malignant ovarian cells. Another study conducted in a large cohort of ovarian cancer patients with 67% having the serous ovarian cancer subtype, showed that only about 7% of HER-2 genes were over-expressed and amplified [36]. Yet, another study delineated that the overall expression of HER-2 in ovarian cancer was about 33%, and that patients with HER-2 positive ovarian tumours had an increased risk of mortality [37].

#### 4.3. Sensitivity of EGFR and HER-2 Positive Cells to Gefitinib and Canertinib

We also show that the anti-tumour effects of gefitinib and canertinib are affected by the levels of EGFR and HER-2 in the ovarian cancer cell line SKOV-3. Furthermore, canertinib shows a greater effect on cell growth and apoptosis than gefitinib in this cell line. Ascitic fluid-derived EGFR positive cells respond to both gefitinib and canertinib, but these responses are distinctive among cell samples. For instance, the measurement of cellular viability is inconsistent among cell samples. The cells that respond to gefitinib also tend to respond to canertinib.

A different scenario is observed in the EGFR and HER-2 positive cells, with only canertinib showing growth inhibitory potential in these cells. However, some cells do not respond to canertinib, even though they have the receptors. This data provides us with valuable information, suggesting that the non-responsiveness of cells to both gefitinib and canertinib could be attributed to additional compensatory pathways that overcome the anti-tumour activities of tyrosine kinase inhibitors (TKIs). However, it should be noted that this study has a small sample size and requires further investigation. Gefitinib has been used extensively to treat non-small cell lung carcinoma (NSCLC), which harbours an EGFR mutant protein [38]. The monotherapy of gefitinib has been evaluated in several trials of other solid tumours of various origins, including cancer of the ovary, but has not shown any effect [21,39–42].

Canertinib is a dual TKI, that has been used as a proof-of-concept compound in many preclinical studies of various tumour types [18,43–45]. Its anti-tumour activities are far superior to the reversible EGFR inhibitor gefitinib. Gefitinib-resistant cancer cells are effectively treated with canertinib in the both wild-type and EGFR mutant cancer cells [46]. However, the anti-tumour activities of canertinib in clinical trials are much less promising. In a phase I clinical trial with canertinib in patients with solid tumours, anti-tumour activity of the inhibitor was notable in only a few individuals [47]. Another phase I clinical evaluation of canertinib in 53 cancer patients did not show any of the objective responses, but the inhibitor down-regulated EGFR, HER-2 and Ki67 [48]. A randomised phase II trial of oral canertinib did not show activity in unscreened patients with advanced ovarian cancer [49].

In our EGFR positive cell populations, both gefitinib and canertinib equally reduced both pERK and pAKT activation. This is, however, rather expected, because both gefitinib and canertinib effectively block EGFR. However, interestingly, some patients with EGFR positive cells do not respond to the inhibitors. It is possible that these cells might have additional pathways that could be activated during the course of the inhibitor treatment. Another plausible explanation is that cells in clusters have a lower cell division rate, and therefore any response to gefitinib and canertinib will be delayed or even non-existent, as these treatments inhibit dividing cells rather than induce apoptosis. In the EGFR and HER-2 positive cells, canertinib shows wider inhibition than gefitinib, especially in the responsiveness of pERK. The decrease in pAKT is also prominent with the canertinib treatment, but this is less than the decrease in pERK.

There are a few preclinical studies investigating the activation of the ERK and AKT signalling pathway in ovarian cancer cells in 3D cell clusters. The non-receptor tyrosine kinase Src is reported to be an essential oncogenic protein that is active in the survival of the mouse ovarian cancer cell line ID-8. Cell aggregates in both in vitro and in vivo conditions of a syngeneic mouse model have activated ERK and AKT via Src activation [26]. Ascitic fluid-derived ovarian cells cultured in 3D

aggregates are more sensitive to AKT inhibitors than similar cells cultured in monolayers, suggesting that floating ovarian cancer cells utilise the AKT activation for survival [50]. In a few ovarian cancer clinical studies, there is no tumour response, but a decrease in phosphorylation of both AKT and ERK has been observed in some patients with an EGFR inhibitor [40,51]. This is in line with our study showing that phosphorylation of ERK and AKT is selectively reduced in ascitic fluid-derived cells after treatment with the inhibitors.

Limitations of the study are that there are no predictable cellular protein markers to determine the sensitivity of gefitinib and canertinib in cell clusters. In addition, the number of cells expressing both EGFR and HER-2 is more responsive to a dual inhibitor canertinib than the EGFR inhibitor gefitinib, which is of a relatively small sample size. This would be interesting if a future study might include more patient samples. The expression of EGFR and HER-2 associated with a patient's survival is not reliable, due to a small number of patients. This, however, could improve if a larger cohort patient might be used in a future study.

## 5. Conclusions

Our study shows that ascitic fluid-derived cells expressing EGFR and HER-2 are more responsive to a dual EGFR and HER-2 inhibitor than the EGFR inhibitor gefitinib. However, these responses are not strongly correlated with the activation of the downstream proteins ERK and AKT. To better understand the effectiveness of canertinib in primary ovarian cancer cells, a robust *in vivo* cell model with a fully functioning immune system is crucial, in order to see whether the inhibitor is specific to cancer cells or immune cells. The *in vivo* model will also better explain the efficacy of the inhibitor and its clinical implications. In addition, some patients are chemo resistant, additional *in vitro* experiments with a combination of chemotherapy and inhibitors would be useful, since the efficacy of small targeted inhibitors would be limited as monotherapy in treatment regimens, and this may greatly influence the molecular profile of cancer cells.

**Author Contributions:** Conducting experiments and analysing data, K.C.; Preparing a manuscript, K.C. and P.S.; Collecting ascitic fluids and obtaining patients' consent, D.H. and B.S. All authors have read and agreed to the published version of the manuscript.

**Funding:** Project was funded by the Ovarian Cancer Research Foundation (OCRF), Melbourne, Australia.

**Acknowledgments:** All ovarian cancer patients who donated ascitic fluid. Judith McKenzie, Haematology Research Group, University of Otago, Christchurch New Zealand for cell lines.

**Conflicts of Interest:** The authors declare no conflict of interest.

## References

1. Ayantunde, A.A.; Parsons, S.L. Pattern and prognostic factors in patients with malignant ascites: A retrospective study. *Ann. Oncol.* **2007**, *18*, 945–949. [[CrossRef](#)]
2. Kim, H.S.; Kim, J.W.; Chung, H.H.; Park, N.H.; Song, Y.S.; Kang, S.B. Disease confined within the ovary and smaller amount of ascites are good prognostic factors for survival of patients with squamous cell carcinoma arising from mature cystic teratoma of the ovary: A case series in Korea and review of the published reports. *J. Obs. Gynaecol. Res.* **2009**, *35*, 99–105. [[CrossRef](#)]
3. Ferriss, J.S.; Java, J.J.; Bookman, M.A.; Fleming, G.F.; Monk, B.J.; Walker, J.L.; Homesley, H.D.; Fowler, J.; Greer, B.E.; Boente, M.P.; et al. Ascites predicts treatment benefit of bevacizumab in front-line therapy of advanced epithelial ovarian, fallopian tube and peritoneal cancers: An NRG Oncology/GOG study. *Gynecol. Oncol.* **2015**, *139*, 17–22. [[CrossRef](#)]
4. Kim, S.; Kim, B.; Song, Y.S. Ascites modulates cancer cell behavior, contributing to tumor heterogeneity in ovarian cancer. *Cancer Sci.* **2016**, *107*, 1173–1178. [[CrossRef](#)]
5. Trachana, S.; Pilalis, E.; Gavalas, N.G.; Tzannis, K.; Papadodima, O.; Liontos, M.; Rodolakis, A.; Vlachos, G.; Thomakos, N.; Haidopoulos, D.; et al. The Development of an Angiogenic Protein "Signature" in Ovarian Cancer Ascites as a Tool for Biologic and Prognostic Profiling. *PLoS ONE* **2016**, *11*, e0156403. [[CrossRef](#)]

6. Kampan, N.C.; Madondo, M.T.; McNally, O.M.; Stephens, A.N.; Quinn, M.A.; Plebanski, M. Interleukin 6 Present in Inflammatory Ascites from Advanced Epithelial Ovarian Cancer Patients Promotes Tumor Necrosis Factor Receptor 2-Expressing Regulatory T Cells. *Front Immunol.* **2017**, *8*, 1482. [[CrossRef](#)]
7. Worzfeld, T.; Strandmann, E.P.; Huber, M.; Adhikary, T.; Wagner, U.; Reinartz, S.; Müller, R. The Unique Molecular and Cellular Microenvironment of Ovarian Cancer. *Front Oncol.* **2017**, *7*, 24. [[CrossRef](#)]
8. Burleson, K.M.; Boente, M.P.; Pambuccian, S.E.; Skubitz, A.P.N. Disaggregation and invasion of ovarian carcinoma ascites spheroids. *J. Transl. Med.* **2006**, *4*, 6. [[CrossRef](#)]
9. Shepherd, T.G.; Thériault, B.L.; Campbell, E.J.; Nachtigal, M.W. Primary culture of ovarian surface epithelial cells and ascites-derived ovarian cancer cells from patients. *Nat. Protoc.* **2006**, *1*, 2643–2649. [[CrossRef](#)]
10. Alvero, A.B.; Chen, R.; Fu, H.; Montagna, M.; Schwartz, P.E.; Rutherford, T.; Silasi, D.; Steffensen, K.D.; Waldstrom, M.; Visintin, I.; et al. Molecular phenotyping of human ovarian cancer stem cells unravel the mechanisms for repair and chemo-resistance. *Cell Cycle* **2009**, *8*, 158–166. [[CrossRef](#)]
11. Bapat, S.A.; Mali, A.M.; Koppikar, C.B.; Kurrey, N.K. Stem and Progenitor-Like Cells Contribute to the Aggressive Behavior of Human Epithelial Ovarian Cancer. *Cancer Res.* **2005**, *65*, 3025–3029. [[CrossRef](#)]
12. Alper, O.; Bergmann-Leitner, E.S.; Bennett, T.A.; Hacker, N.F.; Stromberg, K.; Stetler-Stevenson, W.G. Epidermal growth factor receptor signaling and the invasive phenotype of ovarian carcinoma cells. *J. Natl. Cancer Inst.* **2001**, *93*, 1375–1384. [[CrossRef](#)]
13. Berchuck, A.; Kamel, A.; Whitaker, R.; Kerns, B.; Olt, G.; Kinney, R.; Soper, J.T.; Dodge, R.; Clarke-Pearson, D.L.; Marks, P. Overexpression of HER-2/neu is associated with poor survival in advanced epithelial ovarian cancer. *Cancer Res.* **1990**, *50*, 4087–4091.
14. Steffensen, K.D.; Waldstrom, M.; Andersen, R.F.; Olsen, D.A.; Jeppesen, U.; Knudsen, H.J.; Brandslund, I.; Jakobsen, A. Protein levels and gene expressions of the epidermal growth factor receptors, HER1, HER2, HER3 and HER4 in benign and malignant ovarian tumors. *Int. J. Oncol.* **2008**, *33*, 195–204. [[CrossRef](#)]
15. Miller, V.A. EGFR mutations and EGFR tyrosine kinase inhibitor in non-small cell lung cancer. *Semin. Oncol. Nurs.* **2008**, *24*, 27–33. [[CrossRef](#)]
16. Scartozzi, M.; Bearzi, I.; Berardi, R.; Mandolesi, A.; Pierantoni, C.; Cascinu, S. Epidermal growth factor receptor (EGFR) downstream signalling pathway in primary colorectal tumours and related metastatic sites: Optimising EGFR-targeted treatment options. *Br. J. Cancer* **2007**, *97*, 92–97. [[CrossRef](#)]
17. Prenzel, N.; Zwick, E.; Leserer, M.; Ullrich, A. Tyrosine kinase signalling in breast cancer Epidermal growth factor receptor: Convergence point for signal integration and diversification. *Breast Cancer Res.* **2000**, *2*, 184–190. [[CrossRef](#)]
18. Hassan, W.; Chitcholtan, K.; Sykes, P.H.; Garrill, A. A Combination of Two Receptor Tyrosine Kinase Inhibitors, Canertinib and PHA665752 Compromises Ovarian Cancer Cell Growth in 3D Cell Models. *Oncol. Ther.* **2016**, *4*, 257. [[CrossRef](#)]
19. Hassan, W.; Chitcholtan, K.; Sykes, P.H.; Garrill, A. Ascitic fluid from advanced ovarian cancer patients compromises the activity of receptor tyrosine kinase inhibitors in 3D cell clusters of ovarian cancer cells. *Cancer Lett.* **2018**, *420*, 168–181. [[CrossRef](#)]
20. Montero, J.C.; García-Alonso, S.; Ocaña, A.; Pandiella, A. Identification of therapeutic targets in ovarian cancer through active tyrosine kinase profiling. *Oncotarget* **2015**, *6*, 30057–30071. [[CrossRef](#)]
21. Matsudaa, N.; Lima, B.; Wanga, X.; Uenoa, N.T. Early clinical development of epidermal growth factor receptor targeted therapy in breast cancer. *Expert Opin. Investig. Drugs* **2017**, *26*, 463–479. [[CrossRef](#)] [[PubMed](#)]
22. Francavilla, C.; Lupia, M.; Tsafou, K.; Villa, A.; Kowalczyk, K.; Jersie-Christensen, R.R.; Bertalot, G.; Confalonieri, S.; Brunak, S.; Jensen, L.J.; et al. Phosphoproteomics of Primary Cells Reveals Druggable Kinase Signatures in Ovarian Cancer. *Cell Rep.* **2017**, *18*, 3242–3256. [[CrossRef](#)] [[PubMed](#)]
23. Davidson, B.; Espina, V.; Steinberg, S.; Flørenes, V.A.; Liotta, L.A.; Kristensen, G.B.; GTropé, C.; Berner, A.; Kohn, E.C. Proteomic Analysis of Malignant Ovarian Cancer Effusions as a Tool for Biologic and Prognostic Profiling. *Clin. Cancer Res.* **2006**, *12*, 791–799. [[CrossRef](#)] [[PubMed](#)]
24. Rosso, M.; Majem, B.; Devis, L.; Lapyckyj, L.; Besso, M.J.; Llauro, M.; Abascal, M.F.; Matos, M.L.; Lanau, L.; Castellví, J.; et al. E-cadherin: A determinant molecule associated with ovarian cancer progression, dissemination and aggressiveness. *PLoS ONE* **2017**, *12*, e0184439. [[CrossRef](#)] [[PubMed](#)]

25. Latifi, A.; Luwor, R.B.; Bilandzic, M.; Nazaretian, S.; Stenvers, K.; Pyman, J.; Zhu, H.; Thompson, E.W.; Quinn, M.A.; Findlay, J.K.; et al. Isolation and Characterization of Tumor Cells from the Ascites of Ovarian Cancer Patients: Molecular Phenotype of Chemoresistant Ovarian Tumors. *PLoS ONE* **2012**, *7*, e46858. [[CrossRef](#)]
26. Cai, Q.; Yan, L.; Xu, Y. Anoikis resistance is a critical feature of highly aggressive ovarian cancer cells. *Oncogene* **2015**, *34*, 3315–3324. [[CrossRef](#)]
27. Ho, C.; Chang, S.; Hsiao, C.; Chien, T.; Shih, D.T. Isolation and characterization of stromal progenitor cells from ascites of patients with epithelial ovarian adenocarcinoma. *J. Biomed. Sci.* **2012**, *19*, 23. [[CrossRef](#)]
28. Ó Donnell, R.L.; McCormick, A.; Mukhopadhyay, A.; Woodhouse, L.C.; Moat, M.; Grundy, A.; Dixon, M.; Kaufman, A.; Soohoo, S.; Elattar, A.; et al. The Use of Ovarian Cancer Cells from Patients Undergoing Surgery to Generate Primary Cultures Capable of Undergoing Functional Analysis. *PLoS ONE* **2014**, *9*, e90604.
29. Strauss, R.; Li, Z.; Liu, Y.; Beyer, I.; Persson, J.; Sova, P.; Möller, T.; Pesonen, S.; Hemminki, A.; Hamerlik, P.; et al. Analysis of Epithelial and Mesenchymal Markers in Ovarian Cancer Reveals Phenotypic Heterogeneity and Plasticity. *PLoS ONE* **2011**, *6*, e16186. [[CrossRef](#)]
30. Sodek, K.L.; Ringuette, M.J.; Brown, T.J. Compact spheroid formation by ovarian cancer cells is associated with contractile behavior and an invasive phenotype. *Int. J. Cancer* **2009**, *124*, 2060–2070. [[CrossRef](#)]
31. Suster, N.K.; Smrkolj, S.; Virant-Klun, I. Putative stem cells and epithelialmesenchymal transition revealed in sections of ovarian tumor in patients with serous ovarian carcinoma using immunohistochemistry for vimentin and pluripotency-related markers. *J. Ovarian Res.* **2017**, *10*, 11. [[CrossRef](#)] [[PubMed](#)]
32. Graeff, P.; Crijns, A.P.G.; Hoor, K.A.; Klip, H.G.; Hollema, H.; Oien, K.; Bartlett, J.M.; Wisman, G.B.A.; Bock, G.H.; Vries, E.G.E.; et al. The ErbB signalling pathway: Protein expression and prognostic value in epithelial ovarian cancer. *Br. J. Cancer* **2008**, *99*, 341–349. [[CrossRef](#)] [[PubMed](#)]
33. Lanitis, E.; Dangaj, D.; Hagemann, I.S.; Song, D.-G.; Best, A.; Sandaltzopoulos, R.; Coukos, G.; Powell, D.J. Primary Human Ovarian Epithelial Cancer Cells Broadly Express HER2 at Immunologically-Detectable Levels. *PLoS ONE* **2012**, *7*, e49829. [[CrossRef](#)] [[PubMed](#)]
34. Stadlmann, S.; Gueth, U.; Reiser, U.; Diener, P.; Zeimet, A.G.; Wight, E.; Mirlacher, M.; Sauter, G.; Mihatsch, M.J.; Singer, G. Epithelial growth factor receptor status in primary and recurrent ovarian cancer. *Mod. Pathol.* **2006**, *19*, 607–610. [[CrossRef](#)] [[PubMed](#)]
35. Vermeij, J.; Teugels, E.; Bourgain, C.; Xiangming, J.; in't Veld, P.; Ghislain, V.; Neyns, B.; De Greve, J. Genomic activation of the EGFR and HER2-neu genes in a significant proportion of invasive epithelial ovarian cancers. *BMC Cancer* **2008**, *8*, 3. [[CrossRef](#)] [[PubMed](#)]
36. Tuefferd, M.; Couturier, J.; Penault-Llorca, F.; Vincent-Salomon, A.; Broë, P.; Guastalla, J.; Allouache, D.; Combe, M.; Weber, B.; Pujade-Lauraine, E.; et al. HER2 Status in Ovarian Carcinomas: A Multicenter GINECO Study of 320 Patients. *PLoS ONE* **2007**, *2*, e1138. [[CrossRef](#)]
37. Cai, Y.; Wang, J.; Zhang, L.; Wu, D.; Yu, D.; Tian, X.; Liu, J.; Jiang, X.; Shen, Y.; Zhang, L.; et al. Expressions of fatty acid synthase and HER2 are correlated with poor prognosis of ovarian cancer. *Med. Oncol.* **2015**, *32*, 391. [[CrossRef](#)]
38. Siegel-Lakhai, W.S.; Beijnen, J.H.; Schellens, J.H.M. Current Knowledge and Future Directions of the Selective Epidermal Growth Factor Receptor Inhibitors Erlotinib (Tarceva®) and Gefitinib (Iressa®). *Oncologist* **2005**, *10*, 579–589. [[CrossRef](#)]
39. Leslie, K.K.; Sill, M.W.; Fischer, E.; Darcy, K.M.; Mannel, R.S.; Tewari, K.S.; Hanjani, P.; Wilken, J.A.; Baron, A.T.; Godwin, A.K.; et al. A Phase II Evaluation of Gefitinib in the Treatment of Persistent or Recurrent Endometrial Cancer: A Gynecologic Oncology Group Study. *Gynecol. Oncol.* **2013**, *129*, 486–494. [[CrossRef](#)]
40. Posadas, E.M.; Liel, M.S.; Kwitkowski, V.; Minasian, L.; Godwin, A.K.; Hussain, M.M.; Espina, V.; Wood, B.J.; Steinberg, S.M.; Kohn, E.C. A phase II and pharmacodynamic study of gefitinib in patients with refractory or recurrent epithelial ovarian cancer. *Cancer* **2007**, *109*, 1323–1330. [[CrossRef](#)]
41. Argiris, A.; Ghebremichael, M.; Gilbert, J.; Lee, J.; Sachidanandam, K.; Kolesar, J.M.; Burtness, B.; Forastiere, A.A. Phase III Randomized, Placebo-Controlled Trial of Docetaxel With or Without Gefitinib in Recurrent or Metastatic Head and Neck Cancer: An Eastern Cooperative Oncology Group Trial. *J. Clin. Oncol.* **2013**, *31*, 1405–1414. [[CrossRef](#)] [[PubMed](#)]
42. Patel, S.P.; Kim, K.B.; Papadopoulos, N.E.; Hwu, W.; Hwu, P.; Prieto, V.G.; Bar-Eli, M.; Zigler, M.; Dobroff, A.; Bronstein, Y.; et al. A Phase II Study of Gefitinib in Patients with Metastatic Melanoma. *Melanoma Res.* **2011**, *21*, 357–363. [[CrossRef](#)] [[PubMed](#)]

43. Richards, K.N.; Zweidler-McKay, P.A.; Roy, N.V.; Speleman, F.; Treviño, J.; Zage, P.E.; Hughes, D.P.M. Signaling of ERBB Receptor Tyrosine Kinases Promotes Neuroblastoma Growth in vitro and in vivo. *Cancer* **2010**, *116*, 3233–3243. [[CrossRef](#)] [[PubMed](#)]
44. Irwin, M.E.; Nelson, L.D.; Santiago-O’Farrill, J.M.; Knouse, P.D.; Miller, C.P.; Palla, S.L.; Siwak, D.R.; Mills, G.B.; Estrov, Z.; Li, S.; et al. Small Molecule ErbB Inhibitors Decrease Proliferative Signaling and Promote Apoptosis in Philadelphia Chromosome-Positive Acute Lymphoblastic Leukemia. *PLoS ONE* **2013**, *8*, e70608. [[CrossRef](#)]
45. Dilworth, J.T.; Wojtkowiak, J.W.; Mathieu, P.; Tainsky, M.A.; Reiners, J.J., Jr.; Mattingly, R.R.; Hancock, C.N. Suppression of proliferation of two independent NF1 malignant peripheral nerve sheath tumor cell lines by the pan-ErbB inhibitor CI-1033. *Can Biol. Ther.* **2008**, *7*, 1938–1946. [[CrossRef](#)] [[PubMed](#)]
46. Li, D.; Ambrogio, L.; Shimamura, T.; Kubo5, S.; Takahashi, M.; Chirieac, L.R.; Padera, R.F.; Shapiro, G.I.; Baum, A.; Himmelsbach, F.; et al. BIBW2992, an irreversible EGFR/HER2 inhibitor highly effective in preclinical lung cancer models. *Oncogene* **2008**, *27*, 4702–4711. [[CrossRef](#)]
47. Calvo, E.; Tolcher, A.W.; Hammond, L.A.; Patnaik, A.; de Bono, J.S.; Eiseman, I.A.; Olson, S.C.; Lenehan, P.F.; McCreery, H.; LoRusso, P.; et al. Administration of CI-1033, an Irreversible Pan-erbB Tyrosine Kinase Inhibitor, Is Feasible on a 7-Day On, 7-Day Off Schedule: A Phase I Pharmacokinetic and Food Effect Study. *Clin. Cancer Res.* **2004**, *10*, 7112–7120. [[CrossRef](#)]
48. Zinner, R.G.; Nemunaitis, J.; Eiseman, I.; Shin, H.C.; Olson, S.C.; Christensen, J.; Huang, X.; Lenehan, P.F.; Donato, N.J.; Shin, D.M. Phase I Clinical and Pharmacodynamic Evaluation of Oral CI-1033 in Patients with Refractory Cancer. *Clin. Cancer Res.* **2007**, *13*, 3006–3014. [[CrossRef](#)]
49. Campos, S.; Hamid, O.; Seiden, M.V.; Oza, A.; Plante, M.; Potkul, R.K.; Lenehan, P.F.; Kaldjian, E.P.; Varterasian, M.L.; Jordan, C.; et al. Multicenter, Randomized Phase II Trial of Oral CI-1033 for Previously Treated Advanced Ovarian Cancer. *J. Clin. Oncol.* **2005**, *23*, 5597–5604. [[CrossRef](#)]
50. Correa, R.J.M.; Valdes, Y.R.; Peart, T.M.; Fazio, E.N.; Bertrand, M.; McGee, J.; Préfontaine, M.; Sugimoto, A.; DiMattia, G.E.; Shepherd, T.G. Combination of AKT inhibition with autophagy blockade effectively reduces ascites-derived ovarian cancer cell viability. *Carcinogenesis* **2014**, *35*, 1951–1961. [[CrossRef](#)]
51. Despierre, E.; Vergote, I.; Anderson, R.; Coens, C.; Katsaros, D.; Hirsch, F.R.; Boeckx, B.; Varela-Garcia, M.; Ferrero, A.; Ray-Coquard, I.; et al. Epidermal Growth Factor Receptor (EGFR) Pathway Biomarkers in the Randomized Phase III Trial of Erlotinib Versus Observation in Ovarian Cancer Patients with No Evidence of Disease Progression after First-Line Platinum-Based Chemotherapy. *Target. Oncol.* **2015**, *10*, 583–596. [[CrossRef](#)] [[PubMed](#)]



© 2020 by the authors. Licensee MDPI, Basel, Switzerland. This article is an open access article distributed under the terms and conditions of the Creative Commons Attribution (CC BY) license (<http://creativecommons.org/licenses/by/4.0/>).